Insights into insect wing origin provided by functional analysis of *vestigial* in the red flour beetle, *Tribolium castaneum*

Courtney M. Clark-Hachtel, David M. Linz, and Yoshinori Tomoyasu[1]

Department of Zoology, Miami University, Oxford, OH 45056

Edited by Sean B. Carroll, University of Wisconsin–Madison, Madison, WI, and approved September 6, 2013 (received for review March 6, 2013)

Despite accumulating efforts to unveil the origin of insect wings, it remains one of the principal mysteries in evolution. Currently, there are two prominent models regarding insect wing origin: one connecting the origin to the paranotal lobe and the other to the proximodorsal leg branch (exite). However, neither hypothesis has been able to surpass the other. To approach this conundrum, we focused our analysis on *vestigial* (*vg*), a critical wing gene initially identified in *Drosophila*. Our investigation in *Tribolium* (Coleoptera) has revealed that, despite the well-accepted view of *vg* as an essential wing gene, there are two groups of *vg*-dependent tissues in the "wingless" first thoracic segment (T1). We show that one of these tissues, the carinated margin, also depends on other factors essential for wing development (such as Wingless signal and *apterous*), and has *nubbin* enhancer activity. In addition, our homeotic mutant analysis shows that wing transformation in T1 originates from both the carinated margin and the other *vg*-dependent tissue, the pleural structures (trochantin and epimeron). Intriguingly, these two tissues may actually be homologous to the two proposed wing origins (paranotal lobes and exite bearing proximal leg segments). Therefore, our findings suggest that the *vg*-dependent tissues in T1 could be wing serial homologs present in a more ancestral state, thus providing compelling functional evidence for the dual origin of insect wings.

serial homology | morphological novelty | Hox | appendage evolution

The insect wing is an extremely diverse structure, which has fascinated scientists for centuries. The paranotal hypothesis of insect wing origin proposes that wings evolved from lateral extensions of the notum (the dorsal portion of thoracic body wall), which helped ancient insects to glide and, when eventually articulated, to fly (1, 2; reviewed in refs. 3 and 4) (Fig. 1*B*). The presence of the wing-like paranotal lobes (or winglet) on the first thoracic segment of Paleozoic insects, in addition to similar vein patterning between these lobes and wings, is often used to support this hypothesis (2, 3, 5). The gill or exite hypothesis proposes that insect wings originated from exites (outer leg branches), which stemmed from ancestral proximal leg segments (proximal coxopodites such as epicoxa) (6, 7) (Fig. 1*A*). These ancestral proximal leg segments appear to have fused into the body wall to form the pleural plates in extant insects (5) (Fig. 1*B* and Fig. S1). The exite hypothesis states that these exites evolved into wings, while ancestral proximal leg segments provided a series of sclerotized plates as well as preexisting muscle attachment, allowing the quick acquisition of insect wing articulation (6). Shared expression of some genes between crustacean coxopodite exites and insect wings provides evidence to support the exite hypothesis from an evo-devo point of view (8).

Insect wing development has been studied most thoroughly in a dipteran insect, *Drosophila melanogaster*. These studies have led to an excellent understanding of the molecular basis of the important steps in wing development including induction, differentiation, proliferation, and patterning (see ref. 9 for review). *vestigial* (*vg*), initially identified in *Drosophila*, is an interesting candidate to trace the origin of wing structures. In *Drosophila* embryos, *vg* expression identifies a special set of cells that later becomes the wing disc (10, 11). *vg* is also essential for the proliferation and survival of future wing cells throughout larval development (12), which is exemplified by the *Drosophila vg* null mutant lacking entire wing and haltere structures (13). Proper wing margin formation also depends on *vg* function at the dorsal-ventral (D-V) compartmental border of the wing disc (12). Furthermore, *vg* overexpression in *Drosophila* induces ectopic wing structures, defining *vg* as the wing "master gene" (14). Although the ectodermal function of *vg* in *Drosophila* appears to be specific to wing formation, it is yet to be determined to what extent the function of *vg* is conserved among other insect species. Therefore, analyzing *vg* function in various insects will be useful to gain unique insights into the origin of insect wings.

Results and Discussion

***vg* Function in Wing Development Is Conserved Between *Tribolium* and *Drosophila*.** The wing structures of *Drosophila* and *Tribolium* have become vastly different over evolutionary time. *Drosophila* have flight wings on their second thoracic segment (T2) and modified wing structures, called halteres, on their third thoracic segment (T3) for balance. In contrast, *Tribolium* have modified, hardened protective wing structures on T2, called elytra, and hindwings used for flight on T3 (Fig. 2 *A*, *D*, and *F*). Despite their modification, elytra still maintain wing identity, as disruption of wing genes [such as *vg*, *apterous* (*ap*), and *nubbin* (*nub*)] reduce or remove both wings and elytra in *Tribolium* and other beetles (15, 16).

Significance

Insect wings are a core example of morphological novelty, yet their acquisition remains a biological conundrum. More than a century of debates and observations has culminated in two prominent hypotheses on the origin of insect wings. Here, we show that there are two separate wing serial homologs in the wingless first thoracic segment of a beetle, *Tribolium*. These two tissues are merged to form an ectopic wing structure in homeotic transformation. Intriguingly, the two wing serial homologs may actually be homologous to the two previously proposed wing origins, hence supporting the dual origin of insect wings. The merger of two unrelated tissues may have been a key step in developing this morphologically novel structure during evolution.

Author contributions: C.M.C.-H. and Y.T. designed research; C.M.C.-H., D.M.L., and Y.T. performed research; C.M.C.-H., D.M.L., and Y.T. analyzed data; and C.M.C.-H., D.M.L., and Y.T. wrote the paper.

The authors declare no conflict of interest.

This article is a PNAS Direct Submission.

Freely available online through the PNAS open access option.

Data deposition: The sequence reported in this paper has been deposited in the GenBank database (accession nos. KC688264–KC688267 and KF684967).

[1]To whom correspondence should be addressed. E-mail: tomoyay@miamioh.edu.

This article contains supporting information online at www.pnas.org/lookup/suppl/doi:10.1073/pnas.1304332110/-/DCSupplemental.

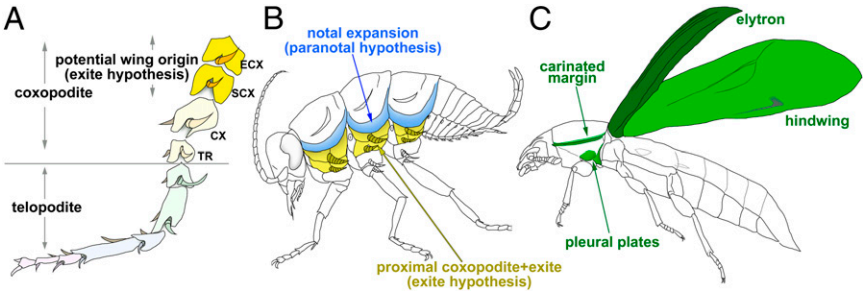

Fig. 1. Two wing origin hypotheses and the combinational wing origin model. (*A*) Arthropod leg ground plan. The proximal coxopodites (ECX and/or SCX) and their exites have been proposed to be a possible wing origin in the gill/exite hypothesis. CX, coxa; ECX, epicoxa; SCX, subcoxa; TR, trochanter. Annotation based on ref. 7. (*B*) The locations of two proposed wing origins (blue and yellow) in an ancestral insect ground plan. Blue, notal expansions; yellow, proximal coxopodites (pleural plates in extant insects) with their exites. (*C*) Wing serial homologs in *Tribolium* (green). The two wing serial homologs in T1 appear to be homologous to two proposed wing origins (blue and yellow tissues in *B*). The merger of these two tissues in *Tribolium* produces ectopic elytra in homeotic transformation, suggesting the combinational wing origin model.

In *Drosophila*, proper wing margin formation depends on *vg* function (12). To investigate whether *vg* is important for wing margin formation in *Tribolium*, we performed *vg* RNAi in the last larval stage. Disruption of *vg* in the last larval stage led to reduction of elytra and hindwings (Fig. 2*B*). The reduction was the result of margin structure deletion, as interior structures and their relative positions remain fairly intact (Fig. 2 *F* and *G* and Fig. S2 *A*–*D*). For example, *vg* RNAi elytra lack marginal hair structures normally present on the wild-type elytra (Fig. S2 *B* and *D*) while retaining intact vein and sensory structure patterns (Fig. S2 *A* and *C*). Similarly, in *vg* RNAi hindwings, the margin structures are deleted while the vein pattern is fairly unaffected (Fig. 2 *F* and *G*). These results indicate that *vg* is responsible for wing margin formation in *Tribolium*.

We next investigated whether the induction and proliferation functions of *vg* are also conserved in *Tribolium*. We disrupted *vg* function in the penultimate stage, just before the onset of wing proliferation. Penultimate *vg* RNAi led to a complete lack of hindwing and elytron discs in the subsequent last larval stage, as well as complete deletion of hindwings and elytra in the resulting adults (Fig. 2*C*). The lack of hindwing and elytron discs during the last larval stages in *vg* RNAi suggests that *vg* plays an important role in the induction of wing structures in *Tribolium*. Alternatively, it is also possible that penultimate *vg* RNAi might be inducing cell death, causing the complete deletion of dorsal appendages.

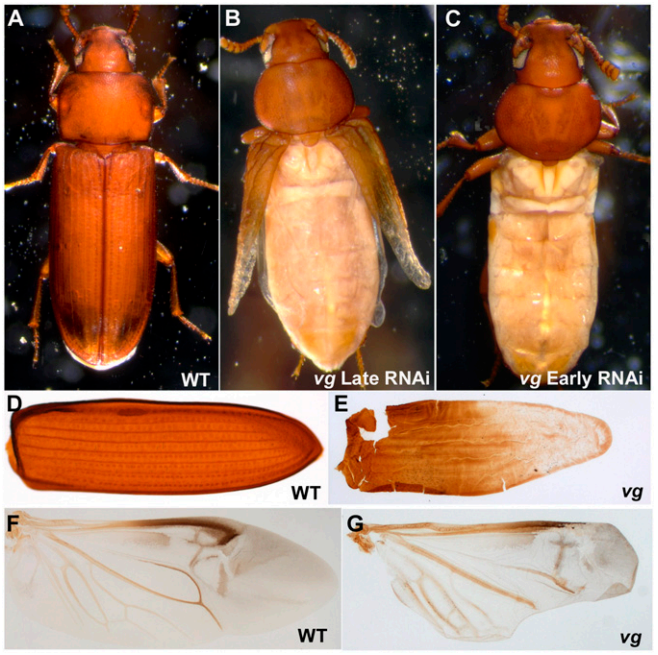

Fig. 2. *vg* is essential for proper wing formation in *Tribolium*. (*A*–*C*) Reduction of wing and elytron in *vg* RNAi. (*A*) Wild type. (*B*) Late *vg* RNAi. (*C*) Early *vg* RNAi. (*D*–*G*) Elytron and hindwing phenotypes caused by *vg* RNAi. (*D* and *F*) Wild type. (*E* and *G*) *vg* RNAi.

***vg* Is Essential for Proper Body Wall Development in *Tribolium*.** Although *vg* has various functions in other tissues (17, 18), *vg* function in the ectoderm appears to be restricted to only dorsal appendage development in *Drosophila* (13). To determine whether the ectodermal function of *vg* is restricted to wing structures in *Tribolium*, we examined the nonwing structures in the *vg* RNAi adults. Interestingly, we noticed several disruptions in the thoracic body wall that were not expected based on previous *Drosophila* studies (Fig. 3). The insect thoracic body wall can be subdivided into three distinct regions; notum or thoracic tergum (dorsal), pleural plates (lateral), and sternum (ventral) (Fig. 3 *A*–*C*). In polyphagan beetles (including *Tribolium*), the dorsal tissue extends ventrally, forming the hypomeron that covers most of the pleural plates (Fig. 3 *A*–*C*; also see Fig. S1) (19, 20). We noticed that *vg* RNAi resulted in a deletion of several pleural plates, one of the trochantin plates (posterior trochantin or trochantin P) and the epimeron, in T1, producing a gap near the base of the T1 leg (Fig. 3 *D*–*F* and *I*–*K*). The other trochantin (anterior trochantin or trochantin A) and the endopleuron were unaffected (Fig. 3 *E* and *J* and Fig. S2*F*). The hypomeron failed to cover the coxa possibly because of the lack of these pleural plates that scaffold the hypomeron from inside (Fig. 3 *E* and *J*). In addition, the lateral ridge of T1 body wall (carinated margin, a part of the dorsal body wall) (20) was missing in the *vg* RNAi beetles (Fig. 3 *G* and *L*). *vg* RNAi also led to the formation of dents on the ventral side of T3 directly above the transverse groove (arrow in Fig. 3 *H* and *M*). This region does not correspond to any previously described structures (20). Although there is no reported function of *vg* in the ectoderm other than wings in *Drosophila*, it is possible that function of *vg* in the body wall may have been overlooked. However, *vg* RNAi in *Drosophila* did not cause any noticeable body wall abnormalities, indicating that *vg* does not hold an important function in adult body wall development in *Drosophila* (Fig. S3). Taken together, these results indicate that *vg* has an important role in the formation of *Tribolium* body wall, a function that is absent in *Drosophila*.

Overlapping of Gene Networks Responsible for Wing and Carinated Margin Development in *Tribolium*. The *vg* RNAi phenotypes in T1 are especially intriguing for several reasons. First, although T1 belongs to the same tagma as the other two thoracic segments, it does not appear to possess wing-related structures (5). The *vg* dependency of the carinated margin and two pleural plates (trochantin P and the epimeron) in T1 may indicate that these tissues are actually related to the wings on T2 and T3 (i.e., serially homologous to wings). Second, these two *vg*-dependent tissues can be homologized to the tissues proposed as the possible sources of wing origin in the two prominent wing origin hypotheses (1, 6) (reviewed in ref. 3). For instance, pleural plates (including the trochantin plates and epimeron) are considered to have originated from the subcoxa, one of the ancestral proximal

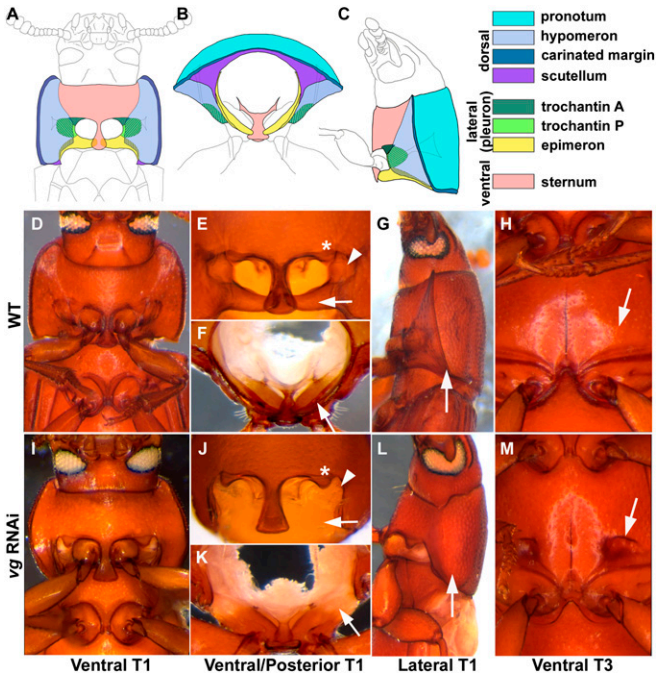

Fig. 3. *vg* RNAi leads to improper body wall formation. (*A–C*) *Tribolium* T1 body wall structures. (*D–H*) Wild type. (*I–M*) *vg* RNAi. Trochantin P (arrowhead in *E* and *J*), the epimeron (arrow in *E, F, J,* and *K*), and the carinated margin (arrow in G and *L*) are affected in *vg* RNAi T1. Trochantin A (asterisk in *E* and *J*) remains unaffected. An arrow in *M* indicates a dent in *vg* RNAi T3.

leg segments that possessed exites (5, 6). The other *vg*-dependent tissue, the carinated margin, is an expansion stemming from the lateral portion of the pronotum. This type of outgrowth is present in many insect orders (5) and appears to be homologous to paranotal lobes. Therefore, it is intriguing that both the carinated margin and the two pleural plates, tissues homologous to two proposed wing origins, are *vg* dependent.

To gain more insight into the relationship between the T1 *vg*-dependent tissues and wings, we next asked whether other wing genes are also responsible for the formation of these tissues. In *Drosophila*, *ap* has the central role in the formation of wings through induction of organizer activity along the D-V boundary (9). The establishment of this D-V organizer is followed by the induction of Wingless (Wg) morphogen, which subsequently patterns wings along the D-V axis (9). The *ap* function in the wing is conserved in *Tribolium*, because depletion of *ap* genes in *Tribolium* causes a similar wing reduction phenotype to that seen in *Drosophila* (there are two *ap* genes in *Tribolium*; ref. 15).

Our RNAi analysis for *ap* genes in *Tribolium* has revealed that *ap* is also important for the formation of the carinated margin. Double RNAi for *apA* and *apB* in the last larval stage resulted in adults with reduced wing and elytron structures as reported (15). Intriguingly, these beetles also lacked the defined carinated margin structure (Fig. 4*B*). In addition, although *apA* single RNAi did not significantly affect wing and elytron structures, it was sufficient to reduce the carinated margin (Fig. S2*G*). In contrast, *apB* RNAi did not produce any noticeable disruption in the carinated margin or wing structures (Fig. S2*H*), suggesting that *ap*A might have a dominant role in the formation of the carinated margin. We also analyzed the pleural plates of the resulting adults; however, we did not detect any noticeable abnormalities caused by *apAB* RNAi.

To further investigate the involvement of wing genes in the carinated margin formation, we performed RNAi to inhibit Wg signal in *Tribolium*. Because there are multiple Wg ligands in *Tribolium* (21), we decided to target *disheveled* (*dsh*) to avoid potential redundancy. *dsh* encodes an intracellular protein that is critical for transducing Wg signal (see ref. 22 to review Wnt pathway). There is only one *dsh* ortholog in *Tribolium* (based on BLAST result), making it an ideal target to inhibit Wg signal through RNAi. RNAi for *dsh* caused multiple defects (such as leg malformation and eye reduction) because of the pleiotropic effect of the Wg signal (Fig. S2 *I* and *J*). Interestingly, the *dsh* RNAi adults lacked the carinated margin structure (Fig. 4*C*). *dsh* RNAi also drastically affected the sternum (the ventral body wall structure), which may represent the conserved function of Wg signal in sternum formation (Fig. S2*J*) (23). Despite the severe reductions in the ventral body wall, the pleural tissues appear to be less affected in these *dsh* RNAi beetles (Fig. S2*J*).

Taken together, these results indicate that there is a significant genetic overlap between wing and carinated margin development, suggesting that the carinated margin and wings may share common ancestry (i.e., are serially homologous). In contrast, we could not find further genetic similarity, other than *vg*, between wings and the pleural plates.

***nubbin* Enhancer Has *vg*-Dependent Residual Activity in the Carinated Margin.** To further investigate the genetic similarity between carinated margins and wings, we have analyzed the involvement of *nub* in the carinated margin development. *nub* is often used as a wing marker (8, 24–26), because of its strong expression that coincides with future wing tissues in *Drosophila* (27). Mutations in *nub* in *Drosophila* cause malformed wings, exemplifying the critical role of *nub* in wing development (27, 28). In *Tribolium*, *nub* is also expressed in the elytron and hindwing discs (15), and RNAi for *nub* induces a reduction of these structures (15). We have analyzed the carinated margin structure in *nub* RNAi beetles; however, we did not detect any abnormality (Fig. S2*K*). Unlike in *Drosophila* (which has two *nub* paralogs; ref. 27), this lack of abnormality cannot be explained by genetic redundancy as *Tribolium* have only one *nub* ortholog in their genome (15). Hence, our *nub* RNAi result indicates that *nub* is not functionally significant in the formation of the carinated margin in *Tribolium*.

Surprisingly, despite the lack of *nub* function in the carinated margin formation, we observed that a *nub* enhancer is active in

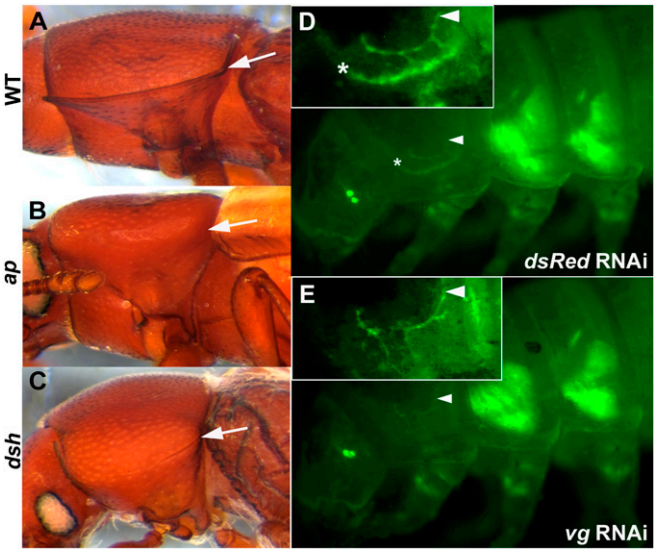

Fig. 4. *ap, dsh*, and the *nub* enhancer are active in the carinated margin formation. (*A–C*) Carinated margin in *ap* and *dsh* RNAi. (*A*) Wild type. (*B*) *apAB* RNAi. (*C*) *dsh* RNAi. Carinated margin is reduced in both *apAB* and *dsh* RNAi (arrows in *B* and *C*). (*D* and *E*) *nub* enhancer activity in the developing carinated margin in *vg* RNAi. (*D*) Control (*dsRed* dsRNA injection). (*E*) *vg* RNAi larvae. *D* and *E Insets* are magnified images of T1. The carinated margin expression (asterisks in *D*) is affected by *vg* RNAi, whereas the neuronal expression (arrowheads in *D* and *E*) remains intact.

the carinated margin during the larval stage. *pu11* is a transgenic line that has a piggyBac transposon containing the 3xP3 enhanced yellow fluorescent protein (EYFP) construct in its genome (29, 30). 3xP3 is an artificial enhancer that drives the downstream gene (EYFP) in both larval and adult eyes (31). In addition to 3xP3, the *pu11* insertion appears to have captured an endogenous enhancer near the insertion site, driving additional EYFP expression in the larval and pupal hindwing and elytron primordia as well as in some neurons (Fig. S4; refs. 29 and 30). Our inverse PCR analysis has revealed that the transposon is inserted near the *nub* locus (Fig. S4). Additionally, the EYFP expression pattern in the hindwing and elytron discs in *pu11* accurately recapitulates the *nub* expression pattern in these tissues (Fig. S4) (15). Thus, *pu11* is likely to be a *nub* enhancer trap line. Upon closer inspection of *pu11* larvae, we noticed that there is a strip of weak EYFP expression in T1 in addition to the strong EYFP expression in the hindwing and elytron discs in T2 and T3. This T1 strip of expression appears to illuminate the future carinated margin (Fig. 4*D*). This expression is transient, visible only in the last 3 d of the last larval stage. The expression is not due to 3xP3 enhancer, because T1 reporter gene expression is absent from other 3xP3 transgenic lines (Fig. S5*A*) and because weak *nub* expression can be detected via in situ hybridization (Fig. S5*B*). Furthermore, *vg* RNAi in the last larval stage eliminated this strip of T1 EYFP expression (Fig. 4*E*), although the nearby neuronal expression remained intact (arrowheads in Fig. 4 *D* and *E*).

These analyses revealed that, although *nub* has no significant function in the carinated margin formation, the *nub* enhancer has residual activity in the future carinated margin. This activity is dependent on *vg*, further illustrating the similarity of the gene networks between the carinated margin and the wing.

Both the Carinated Margin and the Pleural Plates Contribute to the Homeotically Transformed T1 Elytron. Between the two potential wing serial homologs in T1, the carinated margin appears to share more genes (and possibly the interaction among these genes) with wings. To investigate whether the T1 pleural plates are also serially homologous to wing, we have analyzed how these two potential wing serial homologs contribute to the ectopic elytron induced by homeotic transformation. *Sex combs reduced* (*Scr*, or *Cephalothorax*, *Cx*) is the Hox gene that represses wing development in T1 (30). RNAi for *Scr* in *Tribolium* causes a complete transformation of T1 external structures to those of T2 (30). In contrast, an allelic combination of *Cx* (Cx^6/Cx^{apt}, Cx^6 is a null allele of *Scr*, while Cx^{apt} is a hypomorphic allele; refs. 32–34) displays various degrees of transformation (Fig. 5 *D–K* and Fig. S6). Some of the beetles with this allelic combination show fairly complete transformation (Fig. 5 *D–F* and *K*), while others display much weaker transformation (Fig. 5 *G–I*). In the latter individuals, we noticed that the ectopic elytron originates from two distinct places (Fig. 5*I*). One origin of outgrowth occurs at the region close to the carinated margin (white arrow in Fig. 5*I*). In the weakest transformation, the carinated margin appears to be duplicated (or split into two margins), and a new tissue is induced between the two margins (Fig. 5*I*). The tissue interior to the two margins seems to correspond to the dorsal surface of a more completely transformed elytron (Fig. 5 *D–F*). The dorsal portion of the margin bordering this tissue corresponds to the dorsal hinge, while the ventral portion of the margin corresponds to the elytron D-V boundary (white arrow and arrowhead in Fig. 5*I*, respectively). The second outgrowth originates at a more ventral position (black arrow in Fig. 5*I*). Upon close observation, we found that a portion of this outgrowth originates from the base of the epimeron (one of the *vg*-dependent pleural plates) (Fig. 5 *E* and *H*). The epimeron in Cx^6/Cx^{apt} beetles expands laterally between the hypomeron and scutellum to form a part of the ectopic elytron (white arrows in Fig. 5 *E* and *H*). As the dorsal expansion of the epimeron gets larger, the ventral portion of the epimeron is more reduced (asterisks in Fig. 5 *E* and *H*), suggesting that more epimeron cells

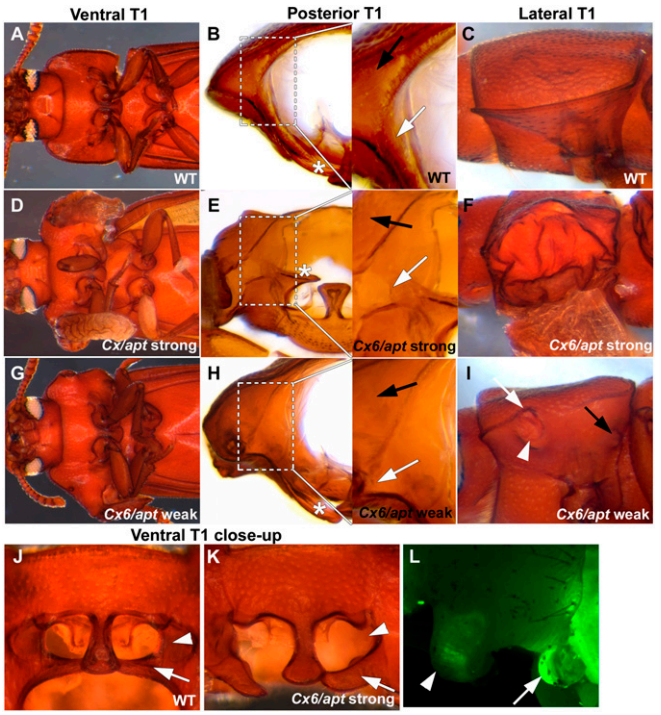

Fig. 5. Reduction of *Scr* leads to elytron-like outgrowths from two distinct regions of T1. (*A–I*) Ectopic elytra on T1. (*A–C*) Wild type. (*D–F*) Cx^6/Cx^{apt} strong. (*G–I*) Cx^6/Cx^{apt} weak. Two distinct outgrowths are most visible in weakly transformed individuals (white and black arrows in *I*). White arrows and arrowheads indicate the dorsal and ventral potion of the split carinated margin, respectively (*I*). (*B, E,* and *H*) The base of the epimeron (white arrow) invades into the space between scutellum (black arrow) and hypomeron, joining the elytron. The epimeron is reduced relative to the degree of transformation (asterisk in *B, E,* and *H*). (*J* and *K*) Reduction of trochantin P (arrowhead) and the epimeron (arrow) in Cx^6/Cx^{apt}. (*J*) Wild type. (*K*) Cx^6/Cx^{apt}. (*L*) *nub* enhancer activity in the carinated margin outgrowth (arrowhead) and the pleural outgrowth (arrow) of Cx^6/Cx^{apt} pupae.

are recruited into the ectopic elytron in the strongly transformed individual. The fate of the *vg*-dependent trochantin in Cx^6/Cx^{apt} beetles is less clear, but it may also be recruited to the ectopic elytron, as the *vg*-dependent trochantin is reduced in the strongly transformed individual (arrowhead in Fig. 5*K*). We have analyzed the *nub* enhancer activity in Cx^6/Cx^{apt} pupae and noticed that both the carinated margin and the pleural outgrowths have EYFP expression (arrowhead and arrow in Fig. 5*L*, respectively), indicating that both outgrowths are *nub* expressing wing-related tissues. Furthermore, the endogenous carinated margin *nub* expression was absent when the outgrowth originating from the carinated margin was present (Fig. S5*C*), suggesting that the carinated margin cells are transforming into the ectopic elytron in Cx^6/Cx^{apt} beetles. In the strongly transformed individuals, the two outgrowths (the carinated margin and pleural outgrowths) are merged into one elytron (Fig. 5 *D–F* and Fig. S6 *G–I*). Although further analysis will be required to decipher the details of this merger, these observations suggest that both the carinated margin and the pleural plates are serially homologous to wings.

Lobes, Gills, Both, or Neither? On the Origin of the Insect Wing. When explaining the structures and development of insect wings, we often state that, in extant insects, wing formation in T1 is "repressed." However, the fate of wing-related tissues in T1 is still elusive. We generally assume that wing-related tissues are never induced in T1. Our findings provide an alternative to this view, in which the wing-related tissues are present in T1, but maintained as (or reverted to) a more "ancestral" state.

Through the *vg* RNAi analysis, we have identified the carinated margin and the two pleural plates as potential wing serial homologs. Between these two groups of tissues, the carinated margin appears to share more genes (and possibly the interaction among these genes) with wings. Then, is the carinated margin the wing serial homolog in T1, not the pleural plates? Two lines of evidence suggest that the two pleural plates may also (at least partially) be serially homologous to wings. First, there are no *vg*-dependent body wall tissues in T2, and they are only residually present in T3 (the region corresponding to the dents induced by *vg* RNAi; Fig. 3*M*). This observation suggests that *vg*-dependent pleural tissues in T2 and T3 are either missing or have been recruited into other tissues, such as wings. The second line of evidence comes from our loss-of-function analysis for *Scr* (*Cx* mutants). We noticed that, in *Tribolium*, both the carinated margin and the pleural plates are transforming into the ectopic T1 elytron. Hence, the wingless T1 has two distinct wing serial homologs: the carinated margin and the pleural plates (Fig. 1*C*).

Recognizing these homologous relationships has a significant impact on our understanding of insect wing origin, as the carinated margin and the pleural plates appear to be homologous to two proposed wing origins (the paranotal lobe and paleozoic proximal leg segments, respectively) (Fig. 1) (1, 3, 5, 6). The shared position of the carinated margin and the paranotal lobe makes it likely that these tissues are homologous. Furthermore, the homologous relationship between ancestral proximal leg segments and pleural plates has also been well supported by fossil and morphological analyses (5, 6). Additionally, our RNAi screening for general developmental toolkit genes in *Tribolium* has identified *odd-skipped* family genes, critical leg genes (35), as an essential factor for pleuron development (Fig. S7), providing further evidence for the proximal leg segment origin of pleural plates. Therefore, although further developmental analysis must be performed to elucidate the evolutionary origin of the pleural plates, our interpretation favors the idea that insect wings have dual origins, namely paranotal lobes and the proximal leg segments.

This is not the first time this type of "combinational model" has been proposed. In fact, both the modified paranotal theory and the revised exite theory propose the dual origin of insect wings (notal expansion+subcoxa in Rasnitsyn, ref. 1; and notal expansion+epicoxa in Kukalova-Peck, ref. 6). More recently, based on expression analysis, Niwa et al. showed that there may be two potential "organ inductive fields" in basal insects and proposed that the fusion of these two fields might be the origin of insect wings (36). Our analysis has revealed a striking similarity in gene networks between wings and notal expansions (i.e., carinated margin) and also provides compelling functional evidence for the dual origin of insect wings.

On the Origin of the Treehopper Helmet. Recently, the helmet of treehoppers, a unique T1 expansion, was proposed to be serially homologous to wings (26). However, later this idea was rebutted, largely because of misinterpretations in the morphological analysis (37, 38). Detailed morphological analysis supports the idea that the treehopper helmet is an extreme posterior expansion of T1 itself (posterior, flattened, cuticular evagination; PFE) instead of an appendage on T1 (37). The widespread tendency for lateral and posterior pronotal expansions in hemipteran insects (such as lace bugs, *Tingidae*) also supports this idea (37). Nonetheless, the genetic similarity between the treehopper helmet and wings (such as *nub* and *Dll* expression) (26) is still remarkable. Miko et al. and Yoshizawa suggested that the genetic similarity was achieved via cooption of wing genes into body wall development (37, 38). Our findings provide yet another possible explanation for the origin of the treehopper helmet. The location of the pronotal expansion in hemipteran insects (at least its lateral portion) appears to correspond to the carinated margin in the beetle T1 (5, 37). Therefore, it is intriguing to speculate that the pads/helmets of hemipteran insects are homologous to beetle carinated margins (but not pleural plates), hence "partially" serially homologous to wings. Gaining (or regaining) some additional wing genes might have allowed hemipteran insects to quickly acquire impressively developed helmet structures. This scenario might also explain the superficial morphological similarities between pronotal pads and wings (such as vein-like structures in lace bugs), because the genetic networks responsible for making these two tissues may share common ancestry. Even bolder speculation can be made regarding the wing-like paranotal lobes of Paleodictyoptera, which were morphologically similar to wings, but lacked elaborate hinge structures (3, 4). These lobes may also have been partially serially homologous to wings. Genetic and developmental analyses in hemipteran insects that possess pronotal expansions (including the helmet of treehoppers) should provide more clues to the origin of these tissues.

Homology Among *vg*-Dependent Tissues. Although identifying homologous structures (both serial homologs in one species and homologs among different species) is crucial to understand the history of morphological evolution, caution must be taken for this kind of homologization. For instance, *vg* function in several different tissues may also be the outcome of independent deployment of *vg* in evolutionarily unrelated tissues (i.e., deep homology via cooption). The extended conservation of the wing gene network in the carinated margin formation, in addition to the homologous positioning of the carinated margin to that of the paranotal lobe, may be used to argue against this possibility. Nonetheless, it will be a challenge to rule out the possibility of cooption. Yet another possibility is an "independent loss" of pleiotropy. It is plausible that *vg* was once important for a large portion of body parts (including wings and body wall), but the *vg* functional domain may have been limited to different regions of the body in different lineages. This scenario would also result in two nonhomologous tissues sharing expression and function of *vg*.

One way to discern homologous structures from linage-specific traits is to analyze multiple lineages. For example, if the *vg* function in T1 we identified in *Tribolium* represents a beetle-unique situation, we would expect to see variations of *vg* function/expression in T1 in different lineages. However, *vg* is expressed in both the edge of terga and the proximal leg segments of a basal

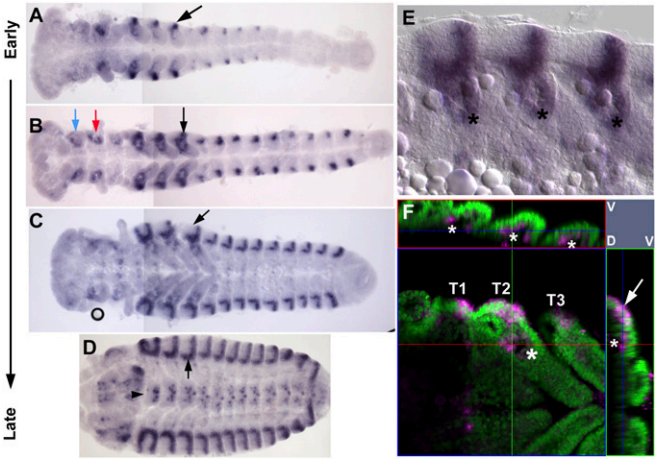

Fig. 6. *vg* expression in the *Tribolium* embryo. (*A–D*) *vg* expression during *Tribolium* embryogenesis. Black arrow denotes T3. Mandible (blue arrow in *B*), maxilla (red arrow in *B*), and central nervous system (arrowhead in *D*) express *vg*. For *A–C*, two images were composed into one to show the whole embryo. (*E*) Close-up of the thoracic region of *C* focused dorsally, showing additional *vg* staining in all three thoracic segments (asterisks). (*F*) Confocal image of *vg* expression (purple) with DAPI nuclear staining (green) in the thoracic segments. Asterisks indicate additional *vg* expression in the thoracic segments dorsal to the leg primordia. Tergal *vg* expression is indicated by an arrow. Dorsal and ventral sides of the image are indicated in the upper right side of *F* by "D" and "V", respectively.

insect (bristletail) (36), which appears to parallel the *vg* function in T1 of *Tribolium.* This observation may further support our interpretation that the wing-related tissues are maintained as (or reverted to) a more ancestral state in the *Tribolium* T1. Tracing the developmental origin of *vg*-dependent structures may also help us evaluate structural homology. Our expression analysis for *vg* has revealed extensive dorsal ectodermal expression of *vg* in the *Tribolium* embryo, which may correspond to the edge of the terga (including the future T1 carinated margin) (Fig. 6 *A–D*). Interestingly, we also identified invaginated *vg*-positive cell populations at the dorsal side of the base of leg primordia in the *Tribolium* embryo (Fig. 6 *E* and *F*). These invaginated "sacks" are found in all three thoracic segments. It would be enlightening to examine how these cells contribute to the pleural plates, the carinated margin, and the wing structures in *Tribolium*. Detailed developmental analysis of the *vg*-dependent structures in *Tribolium*, as well as other insect and arthropod species, should provide unique insights into the origin of insect wings.

While this manuscript was under review, Ohde et al. reported that the hypomeron in T1 and gin traps in the pupal abdominal segments are wing serial homologs in another beetle, *Tenebrio molitor* (39). Their finding of wing serial homologs in nonwinged segments, together with our detailed identification of T1 wing homologs, the carinated margin (a specific part of the hypomeron) as well as nonhypomeron structures such as the pleural plates, will further our understanding of insect wing origin and diversification.

Materials and Methods

Insect Cultures. Beetles were cultured on whole wheat flour [+5% (wt/wt) yeast] at 30 °C. Detailed genotypes of the beetles and flies used in this study are in *SI Materials and Methods*.

Gene Cloning, dsRNA Synthesis, and RNAi. Injection and dsRNA synthesis were performed as described (40). Detailed information including primer sequences, inverse PCR, RACE, off-target effect assessment, and GenBank accession numbers are in *SI Materials and Methods* and Table S1.

Tissue Staining and Documentation. In situ hybridization was performed as described (15). The images were captured by using Zeiss AxioCam MRc5 with AxioPlan 2 or Zeiss Discovery V12. Confocal images were captured by using Zeiss 710. Detailed tissue dissection and fixation procedures are in *SI Materials and Methods*.

ACKNOWLEDGMENTS. We thank R. Beeman, S. Haas, and K. Leonard for *Cx* mutants; Bloomington Stock Center and Vienna Drosophila RNAi Center for fly stocks; the Center for Bioinformatics and Functional Genomics and Center for Advanced Microscopy and Imaging at Miami University for technical support; J. Parker for helpful comments; P. Ravisankar and H. Steigelman for technical assistance; and members of Y.T. laboratory for discussion. This work was supported by a Miami University start-up grant (to Y.T.) and National Science Foundation Grant IOS 0950964 (to Y.T.).

1. Rasnitsyn AP (1981) A modified paranotal theory of insect wing origin. *J Morphol* 168:331–338.
2. Hamilton KGA (1971) The insect wing, Part 1. Origin and development of wings from notal lobes. *J Kans Entomol Soc* 44:421–433.
3. Grimaldi D, Engel MS (2005) *Insects Take to the Skies. Evolution of the Insects* (Cambridge Univ Press, New York), pp 155–187.
4. Kukalova-Peck J (1991) Fossil history and the evolution of hexapod structures. *The Insects of Australia: A Textbook for Students and Research Workers*, ed Naumann ID (Melbourne Univ Press, Carlton, Australia), 2nd Ed, Vol 1, pp 141–179.
5. Snodgrass RE (1935) *The Thorax. Principles of Insect Morphology* (Cornell Univ Press, New York), pp 157–192.
6. Kukalova-Peck (1983) Origin of the insect wing and wing articulation from the arthropodan leg. *Can J Zool* 61:1618–1669.
7. Kukalova-Peck J (2008) Phylogeny of higher taxa in insecta: Finding synapomorphies in the extant fauna and separating them from homoplasies. *Evol Dev* 35:4–51.
8. Averof M, Cohen SM (1997) Evolutionary origin of insect wings from ancestral gills. *Nature* 385(6617):627–630.
9. Brook WJ, Diaz-Benjumea FJ, Cohen SM (1996) Organizing spatial pattern in limb development. *Annu Rev Cell Dev Biol* 12:161–180.
10. Cohen B, Simcox AA, Cohen SM (1993) Allocation of the thoracic imaginal primordia in the Drosophila embryo. *Development* 117(2):597–608.
11. Goto S, Hayashi S (1997) Specification of the embryonic limb primordium by graded activity of Decapentaplegic. *Development* 124(1):125–132.
12. Zecca M, Struhl G (2007) Control of Drosophila wing growth by the vestigial quadrant enhancer. *Development* 134(16):3011–3020.
13. Williams JA, Bell JB, Carroll SB (1991) Control of Drosophila wing and haltere development by the nuclear vestigial gene product. *Genes Dev* 5(12B):2481–2495.
14. Halder G, et al. (1998) The Vestigial and Scalloped proteins act together to directly regulate wing-specific gene expression in Drosophila. *Genes Dev* 12(24):3900–3909.
15. Tomoyasu Y, Arakane Y, Kramer KJ, Denell RE (2009) Repeated co-options of exoskeleton formation during wing-to-elytron evolution in beetles. *Curr Biol* 19(24): 2057–2065.
16. Ohde T, et al. (2009) Vestigial and scalloped in the ladybird beetle: A conserved function in wing development and a novel function in pupal ecdysis. *Insect Mol Biol* 18(5):571–581.
17. Deng H, Bell JB, Simmonds AJ (2010) Vestigial is required during late-stage muscle differentiation in Drosophila melanogaster embryos. *Mol Biol Cell* 21(19):3304–3316.
18. Guss KA, Mistry H, Skeath JB (2008) Vestigial expression in the Drosophila embryonic central nervous system. *Dev Dyn* 237(9):2483–2489.
19. Hlavac TF (1972) The prothorax of Coleoptera: Origin, major features of variation. *Psyche (Stuttg)* 79(3):123–149.
20. El-Kifl (1953) Morphology of the adult Tribolium confusum Duv. and its differentiation from Tribolium (Stene) castaneum Herbst. *Bulletin de la Société Fouad Ier d'Entomologie* 37:173–249.
21. Bolognesi R, et al. (2008) Tribolium Wnts: Evidence for a larger repertoire in insects with overlapping expression patterns that suggest multiple redundant functions in embryogenesis. *Dev Genes Evol* 218(3-4):193–202.
22. Logan CY, Nusse R (2004) The Wnt signaling pathway in development and disease. *Annu Rev Cell Dev Biol* 20:781–810.
23. Shirras AD, Couso JP (1996) Cell fates in the adult abdomen of Drosophila are determined by wingless during pupal development. *Dev Biol* 175(1):24–36.
24. Damen WG, Saridaki T, Averof M (2002) Diverse adaptations of an ancestral gill: A common evolutionary origin for wings, breathing organs, and spinnerets. *Curr Biol* 12(19):1711–1716.
25. Jockusch EL, Ober KA (2004) Hypothesis testing in evolutionary developmental biology: A case study from insect wings. *J Hered* 95(5):382–396.
26. Prud'homme B, et al. (2011) Body plan innovation in treehoppers through the evolution of an extra wing-like appendage. *Nature* 473(7345):83–86.
27. Ng M, Diaz-Benjumea FJ, Cohen SM (1995) Nubbin encodes a POU-domain protein required for proximal-distal patterning in the Drosophila wing. *Development* 121(2): 589–599.
28. Cifuentes FJ, García-Bellido A (1997) Proximo-distal specification in the wing disc of Drosophila by the nubbin gene. *Proc Natl Acad Sci USA* 94(21):11405–11410.
29. Lorenzen MD, et al. (2003) piggyBac-mediated germline transformation in the beetle Tribolium castaneum. *Insect Mol Biol* 12(5):433–440.
30. Tomoyasu Y, Wheeler SR, Denell RE (2005) Ultrabithorax is required for membranous wing identity in the beetle Tribolium castaneum. *Nature* 433(7026):643–647.
31. Berghammer AJ, Klingler M, Wimmer EA (1999) A universal marker for transgenic insects. *Nature* 402(6760):370–371.
32. Beeman RW, Stuart JJ, Haas MS, Denell RE (1989) Genetic analysis of the homeotic gene complex (HOM-C) in the beetle Tribolium castaneum. *Dev Biol* 133(1):196–209.
33. Curtis CD, et al. (2001) Molecular characterization of Cephalothorax, the Tribolium ortholog of Sex combs reduced. *Genesis* 30(1):12–20.
34. Shippy TD, Rogers CD, Beeman RW, Brown SJ, Denell RE (2006) The Tribolium castaneum ortholog of Sex combs reduced controls dorsal ridge development. *Genetics* 174(1):297–307.
35. Hao I, Green RB, Dunaevsky O, Lengyel JA, Rauskolb C (2003) The odd-skipped family of zinc finger genes promotes Drosophila leg segmentation. *Dev Biol* 263(2):282–295.
36. Niwa N, et al. (2010) Evolutionary origin of the insect wing via integration of two developmental modules. *Evol Dev* 12(2):168–176.
37. Mikó I, et al. (2012) On dorsal prothoracic appendages in treehoppers (Hemiptera: Membracidae) and the nature of morphological evidence. *PLoS ONE* 7(1):e30137.
38. Yoshizawa K (2012) The treehopper's helmet is not homologous with wings (Hemiptera: Membracidae). *Syst Entomol* 37:2–6.
39. Ohde T, Yaginuma T, Niimi T (2013) Insect morphological diversification through the modification of wing serial homologs. *Science* 340(6131):495–498.
40. Philip BN, Tomoyasu Y (2011) Gene knockdown analysis by double-stranded RNA injection. *Methods Mol Biol* 772:471–497.